IWEC – Model Validation and Cost Optimization of InfinityWEC Wave Energy Converter

A. Rashid, M. Sidenmark, C. Eskilsson and M. Wallentin

Abstract— **This paper presents the methods developed and key findings of the IWEC project performed by Ocean Harvesting Technologies AB (OHT). It aimed to reduce the levelized cost of energy (LCoE) of OHT's wave energy converter InfinityWEC, by analysing how different key parameters impact cost and annual output using a model of a 100-MW array installation. Component-level cost functions were developed and mapped to key parameters and constraints of the system. A large number of system configurations were then evaluated with a numerically efficient 3 degree-of-freedom (DoF) nonlinear radiation-diffraction model in WEC-Sim along with OHT's sea state-tuned polynomial reactive control (PRC). The most promising configurations were identified and investigated in more detail. The configuration with the best LCoE were finally identified and analysed further, including estimation of the effect of changing the PRC to model predictive control, which resulted in 17-34% higher annual output and 12-23% lower LCoE. The final LCoE was found to be 93 – 162 EUR / MWh at 100 MW installed capacity. An important finding from the study is that using simplified metrics such as CAPEX/ton was found to be irrelevant. Numerical wave tank testing, high-fidelity computational fluid dynamics (CFD), were used to tune the viscous drag of the 3 DoF WEC-Sim model. Applying verification and validation (V&V) techniques the CFD simulations showed a relatively large numerical uncertainty, but the average power and the motion responses were found to be sufficiently accurate.**

Keywords—**Wave power, LCoE, Techno-economic optimization, numerical wave tank testing, CFD, model validation**

This work was supported in part by the Swedish Energy Agency under grant 47398-1.

A. Rashid works at Ocean Harvesting Technologies AB, Campus Gräsvik 28, SE-37175 Karlskrona, Sweden (e-mail: ahmed.rashid@oceanharvesting.com).

M. Sidenmark works at Ocean Harvesting Technologies AB, Campus Gräsvik 28, SE-37175 Karlskrona, Sweden (e-mail: ahmed.rashid@oceanharvesting.com).

C. Eskilsson is with the Renewable Energy Unit at Research Institutes of Sweden (RISE), Box 857, SE-50115 Borås, Sweden (e-mail: claes.eskilsson@ri.se).

M. Wallentin works at Ocean Harvesting Technologies AB, Campus Gräsvik 28, SE-371 75 Karlskrona, Sweden, (e-mail: markus.wallentin@oceanharvesting.com).

I. Introduction

A major challenge for wave power is to show an energy production cost that enables establishment on the market in competition with other energy types. Many WEC technologies have been tested in different scale at sea, but the energy production cost has been high and the commercial break through is still yet to come. There is a need for early-stage concept evaluation and design optimization, using numerical simulations to assess performance and balance key system parameters to minimize the LCoE. Dry and wet testing of physical prototypes should be done first when a clear path to economic viability has been shown, with focus on validating the design, survivability, performance and to validate and calibrate the simulation models for the next stage of the technology development and validation.

Studies have been done to assess and benchmark the techno-economic performance of different wave energy technologies, [1]-[3]. Most of these studies have utilized key metrics such as annual energy capture per physical quantities, such as mass, force or volume. However, the relevance or correlation of these key metrics to LCoE is very questionable. As an example, the weight-to-cost is highly varying for different components and structures in the system, depending on the material and manufacturing processes, to the extent that it can be very misleading if used in a techno-economic optimization study.

Therefore, there is need to 1) develop cost functions on a component level to estimate the overall cost of the system for different combinations of system parameters, 2) run simulations for each system configuration individually and calculate the annual energy output and 3) optimize the system configuration with the objective to minimize LCoE.

OHT has recently completed the IWEC project, which developed a methodology to minimize the LCoE based on component level cost estimation and assessment of the impact on overall cost by varying key system parameters, along with performance assessment using numerical simulation models calibrated with numerical tank tests. This papers presents the outcome from applying this methodology on the InfinityWEC, and the methods can be used also for other WEC designs to perform LCoE based cost optimization through all development stages.

 Copyright © European Wave and Tidal Energy Conference 2021

II. THE INFINITYWEC SYSTEM

InfinityWEC is a novel point absorbing wave energy converter (WEC), that comprises of a modular hull design and a direct-drive electromechanical PTO system, see Fig. 1 and Fig. 2. The WEC is split into two main pieces that are connected with a tether line, denoted upper tether: 1) a floater, denoted buoy, and 2) a submerged hull, denoted PTO hull, that encapsulates the complete PTO. The upper tether lowers the moment loads ideally to zero, while the split design of the hulls enables efficient construction and simplifies transportation and installation.

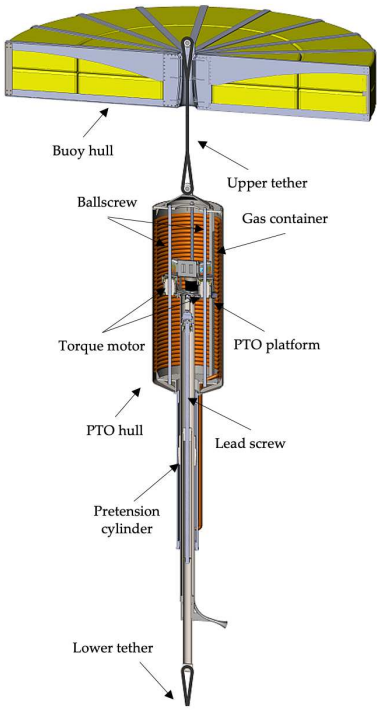

Fig. 1. Cut view of the InfinityWEC wave energy converter.

In the presented analyses, the PTO comprises of a modular ball screw actuation system, connected to frameless torque motors, a lead screw level adjustment system and a pneumatic pretension system, comprising of a pneumatic cylinder connected to a large, pressurized gas volume. The PTO is held in a fixed vertical position by the mooring system while the non-rotating ball screws attached to the PTO hull are pushed up and down through the PTO platform, when the buoy is set in motion by the waves. The lead screw connects the PTO platform to the lower mooring system and is used to adjust the height of the PTO for tidal variations and to submerge the WEC to secure survival in storm conditions. The pretension system provides a nearly constant force, which keeps the mooring tensed, thus enabling electricity to be produced in both directions. The lead screw actuator is placed inside the hollow piston rod of the pretension cylinder to minimize the total height of the WEC. Due to its direct-drive nature, with the integrated ball screw torque motor units, the system provides advanced force control to maximize the energy production while considering constraints essential for a cost effective and reliable system.

The design of the system has been further refined since this study was done but the overall function remains the same.

III. METHOD

A. Overview

A full system design of a wave farm has been evaluated including the electrical infrastructure and a power cable to land for grid connection. Main system parameters, such as tether force, stroke length, root-mean-square (RMS) power, dimensions and mass of the buoy were first identified for the optimization study. Then cost functions is developed for each component, which relates the optimization parameters to the overall cost of the system. This is done based on input from suppliers, component cost models in the literature [4] and company experience. To minimize the number of performed simulations, a set of sea states is chosen to represent the whole wave scatter. A parametric study is then made in which the weighted average power from the selected set of sea states is valued against the computed cost for each configuration. The three configurations with the highest score for different width of the buoy is then selected and the annual energy production is calculated based on 6 different wave scatters. From that, an optimal system configuration, defined in terms of lowest LCoE, is found.

The system configurations are evaluated with a nonlinear 3 DoF simulation model in WEC-Sim using the

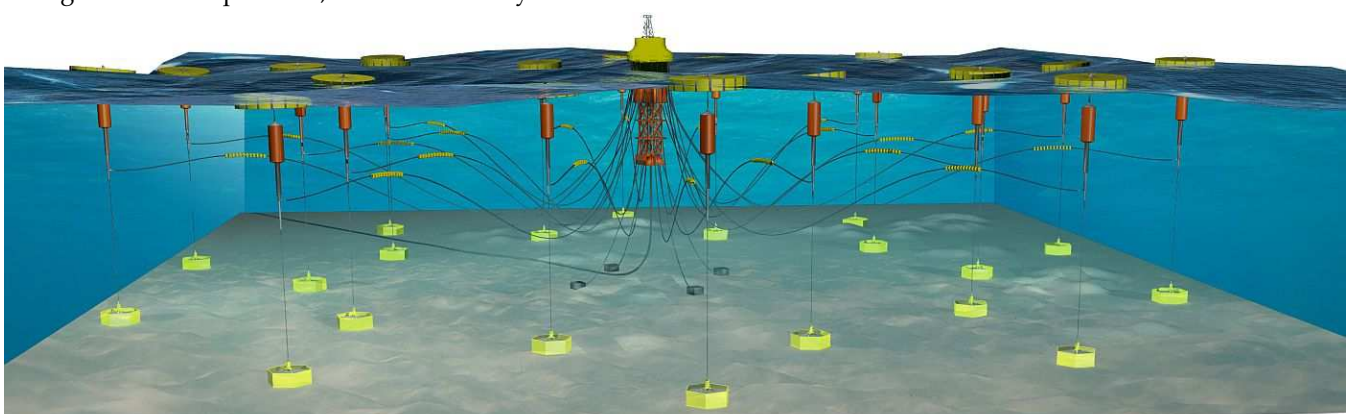

Fig. 2. Cluster of InfinityWECs with a central floating substation.

sea state tuned polynomial reactive control (PRC), presented in [5]. To increase the accuracy of the produced results, the 3 DoF drag coefficients used in the WEC-Sim model is calibrated against high-fidelity CFD simulations in a numerical wave tank (NWT) testing set-up, using a set of drag identification experiments. The spatial discretization uncertainty in CFD simulations is estimated with a V&V methodology. Due to the vast computational cost of performing CFD simulations, drag calibration is performed only on a base system configuration prior to performing the optimization study. This set of drag coefficients is used for all system configurations throughout the optimization study. Finally, the drag coefficients are re-calibrated for the optimized configuration and compared against the once used during the optimization study.

The study ends with an evaluation of the potential performance improvement and LCoE reduction of the optimal buoy configuration, using model predictive control with 5 second wave prediction to optimize the PTO force.

B. Optimization Methodology

In this study, a two-stage optimization methodology is used. The first stage identifies the configuration that maximizes the weighted average power from a set of representative sea states per total cost of goods (CoGs) for each of the studied buoy widths. At the second stage annual simulations are run to calculate LCoE in the selected wave climates for each optimal buoy configuration from the first stage. The optimal configuration in terms of lowest LCoE for an array installation of 100 MW is then found.

C. Average Power Evaluation

To calculate the average power output for a full year in a given location, one ideally needs to simulate each sea state in the scatter to extract the average output power in each sea state. However, doing so would result in too large simulation effort, making it impossible to complete the optimization study within the time frame of the project. To minimize the number of performed simulations, five sea states sweeping diagonally across the scatter are chosen to represent the whole wave scatter. Using the average power computed with the base configuration, and the number of hours of occurrences of the selected set of sea states, a weight for each sea state is obtained. This weight is used to give an estimate of the average power of the whole scatter by computing a weighted average power of the selected sea states. The selected sea states together with their computed weights for each sea scatter is presented in Table I. Note that one can use larger number of sea states to get a better estimate of the average power output.

TABLE I
WEIGHTING OF SELECTED SEA STATES FOR EACH WAVE SCATTER

	HB[a]	PZ	LB	BM	NS	BC
Hs=1.75m Te=6.5s	16%	21%	42%	10%	30%	20%
Hs=2.75m Te=7.5s	28%	69%	53%	23%	38%	25%
Hs=3.75m Te=8.5s	30%	11%	5%	24%	24%	18%
Hs=4.75m Te=9.5s	18%	0%	0%	23%	5%	13%
Hs=5.75m Te=10.5s	8%	0%	0%	19%	3%	24%

[a] Sites and their abbreviations are summarized in Table II.

D. CAPEX Calculation

The CAPEX calculation is performed using the pricing in a CoGs list based on supplier quotes for 100 units of the base configuration. To estimate cost for a new configuration, a cost model is developed. The cost is scaled individually for each cost item, depending on how it is affected by each of the considered parameters relative to the base configuration. The scaling model for CoGs item j is

$$c_{n_j} = c_{b_j} \prod_{i=1}^{n} \left(1 - \left(1 - \frac{p_{n_i}}{p_{b_i}}\right)\sigma_{ij}\right) \tag{1}$$

where c_{n_j} and c_{b_j} are the cost of item j with the new and the base configuration respectively, p_{n_i} and p_{b_i} are the values of the ith cost-driving parameter with the new and the base configuration respectively and $\sigma_{ij} \in \{0, 1\}$ is a scaling factor, that shows the dependence of the CoGs item j on parameter i. The total CAPEX is the sum of all CoGs and the cost for installation, which is assumed to be 15% of the sum of all CoGs, [6].

The cost-driving parameters are the optimization parameters presented in Table IV but also their derivatives such as the tether force, which is dimensioning the mooring and the level system, and computed quantities such as RMS output power, which is relevant for the cost of electrical equipment. The scaling factor is equal to 0, when a CoG item j does not directly depend on parameter i, and it is a positive value less than or equal to 1, when there is a dependency. For example, the ball screw cost does not depend on buoy mass and volume, but it depends on maximum PTO force and the stroke length.

For the electrical system, the topology of each configuration is needed to calculate total cable length and the total number of electrical components in the electrical infrastructure, such as transformers and switchgears. This is done by finding the number of buoys and clusters required to achieve the design array rating of 100MW for each configuration. The Lundberg model [4], for costs have been used for the dynamic power cable, switch gear and high voltage transformer. Lundberg's models are obtained by fitting analytical curves to supplier cost data of different components with different ratings. However, the parametrization is done by component cost data from 2003. Hence, the cost parameters are adjusted to today's

(2020) prices using an average annual inflation rate of 2%. Lundberg's model for power cables is an exponential function of rated power, while the different coefficients in the model depend on the rated voltage. The switch gear cost model is a linear function of rated voltage, and high voltage transformer model is a power function of rated power. Since the voltage levels at different locations of the array do not differ with respect to the system configurations, the electrical system is priced based on the RMS electrical power through the system. The power factor throughout the electrical system is assumed to be 1. Using RMS power and not the peak power as the sizing parameter is an assumption that was made for this study, since most electrical components in general can handle short-term overloading without overheating. But the thermal time constant varies between different components, and for some components it may be more appropriate to use peak power. RMS power from each cluster and the total array have been calculated with the same design sea-state wave profile and a time delay to each WEC according to the topology and speed of the wave propagation, with the waves approaching from top to bottom in Fig. 4. This angle is selected since it gives the highest variations in the collected power, which is important for the sizing of the array cables.

E. Learning Curve Model and LCoE Calculation

To obtain the n:th unit cost for an installation of 100 MW array, the widely used learning curve methodology is applied. It states that every time the volume of a product is doubled, the cost is reduced by a learning rate. It yields,

$$CAPEX_{n:th} = CAPEX_1 n^{log_2 \gamma} \tag{2}$$

where γ is the learning rate chosen to 82%, with reference to [3].

The LCoE is calculated as the ratio between the discounted sum of costs and the discounted sum of the energy production over the lifetime of the plant:

$$LCoE = \frac{\sum_{t=1}^{n} \frac{(CAPEX_t + M_t + I_t)}{(1+r)^t}}{\sum_{t=1}^{n} \frac{E_t}{(1+r)^t}} \tag{3}$$

where n is the lifetime of the plant, which is designed to be 20 years, $CAPEX_t$ is the capital expenditure for year t, M_t is the operations and maintenance cost, I_t is the insurance costs, E_t is the energy yield and r is the discount rate, which is set to 10%, matching the Ocean Energy Systems LCoE model [7].

Since the CoGs represent the average cost of 100 WEC devices, the first unit cost in the learning curve is tuned so that the accumulated average cost at 100 units match the CoGs, after which the n:th unit cost at 100 MW installed capacity can be derived.

In this project it is assumed that the total CAPEX for the whole array installation occurs during the first year, the operations and maintenance cost per year is 6% of the CAPEX, insurance cost per year is 2% of the CAPEX and the energy yield per year is constant throughout the lifetime of the project.

F. Numerical Wave Tank

Nonlinear radiation-diffraction models are usually the preferred choice for power production analysis due to their computational efficiency. However, due to the underlying assumptions in their formulation, the accuracy of these kind of models can be low, especially when energy-maximizing control strategies are applied. Therefore, these models are usually validated and calibrated using physical water laboratory test [8] or numerical wave tank (NWT) testing using CFD [9]. NWT testing allows validation of any geometry to be done at full-scale, avoids common issues encountered in physical tank testing, such as reflecting waves, and is generally a cost-effective solution when it comes to model validation. Due to these benefits, NWT testing is the applied validation method in this study.

To judge the reliability and assess the uncertainty of the numerical solution, formal V&V techniques are effectively applied in this work. The procedure is based on Richardson extrapolation, as proposed in [10]. To obtain the numerical uncertainties a series of minimum four grids with different grid density is needed. The methodology and expressions for calculating the uncertainties can be found in [10].

G. Drag identification

The tuning of the drag coefficients is performed by the nonlinear gradient-based algorithm, *fmincon,* in MATLAB. Drag coefficients are initially optimized with a motion objective to minimize the combined least square error from all DoFs between the motion responses in CFD and WEC-Sim. Due to the different amplitudes of the position response for each DoF, the signals both in WEC-Sim and CFD are normalized by the maximum absolute amplitudes of signals in CFD. The motion objective function is then expressed as

$$\min_{C_d} \sum_i \frac{\left\| x_{cfd_i} - x_{wecsim_i} \right\|_2^2}{\left\| x_{cfd_i} \right\|_\infty^2} \tag{4}$$

where $i = \{1, 3, 5\}$ is the index to denote the DoF, x_{cfd} and x_{wecsim} are respectively the CFD and WEC-Sim responses and the operators $||.||_2$ and $||.||_\infty$ represent respectively the Euclidean norm and the maximum norm.

It was observed that the motion objective underestimates the performance with respect to WEC-Sim. Thus, the drag coefficients are also tuned for the final configuration with a power objective that minimizes

the error in mean output power between CFD and WEC-Sim.

IV. DATA

A. Environmental conditions

In this project, analysis is performed using wave scatters from six different locations, which are listed in Table II together with the abbreviations used in the paper and the available wave resource in them. The sea floor for all locations is assumed to be flat with constant water depth of 50 meters. Moreover, the waves are assumed to be unidirectional.

TABLE II
WAVE SITES AND THEIR ABBREVIATIONS

Wave site	Abbreviation	Resource [kW/m]
Haltenbaken	HB	42
Pilot zone	PZ	25
Lisboa	LB	37
Belmullet	BM	72
North Sea	NS	20
Billia Cro	BC	24

B. Base configuration

Starting point for the optimization study is the base configuration of the InfinityWEC presented in Table III.

TABLE III
BASE CONFIGURATION PARAMETER VALUES

Property	**Parameter**	**Value**	**Unit**
Diameter	d_b	15	m
Height	h_b	2.14	m
Volume	V_b	378	m^3
Mass	m_b	84.3×10^3	kg
Center of gravity	z_{cg}	-0.305	m
Pitch inertia	I_{yy}	1.068×10^6	kgm^2
Mooring pretension	F_{pre}	1.5×10^6	N
Maximum control force	F_{max}	1.5×10^6	N

C. Configuration for the Optimization Study

Main system parameters for the optimization study have been identified based on their impact on power output performance and cost. They are summarized in Table IV, with their evaluated range and increment step.

TABLE IV
SYSTEM CONFIGURATIONS FOR OPTIMIZATION STUDY

Optimized parameters	Min	Max	Step	Unit
Buoy diameter	9	15	3	m
Maximum control force	1	2	0.5	MN
Maximum stroke	4	7	1	m
Volume	350	750	50	m^3
Mass	25	275	25	ton

It was observed that the performance of the buoy degraded significantly if the buoy volume was chosen smaller in relation to the buoy mass and total PTO force. Moreover, the device performance converged with increasing the total buoy volume in relation to the buoy mass and total PTO force. Finally, combinations with small volume and large diameter are excluded due to the increased occurrence of nonlinear phenomena such as overtopping, which cannot be accurately captured by WEC-Sim. Therefore, the minimum and maximum swept volume were chosen individually for each combination of buoy mass, width, and total PTO force, see Table XII for simulated combinations. Nevertheless, the buoy still got submerged in larger waves and the WEC-SIM results should be treated with care.

D. Array Layout

A cluster topology in a pattern, as shown in Fig. 3, is used for the array layout. Each cluster consists of 12 WECs, connected with a dynamic power cable to the PTO hull. The dynamic cables go directly to the substation without touching the seabed. The cables from the substation of each cluster have a dynamic part down to the seabed, where it is permanently spliced onto a static string cable. Each substation connects directly to a master substation, which contains the high voltage transformer and land cable connection. Switchgears are available to allow isolation of each individual buoy, each individual cluster and the complete array.

The total number of cluster and buoys depends on the rating of a single WEC, which in turn depends on the system configuration. WEC spacing is based on the simulated surge motion with an added margin of 20% to give room for installation and retrieval of WECs.

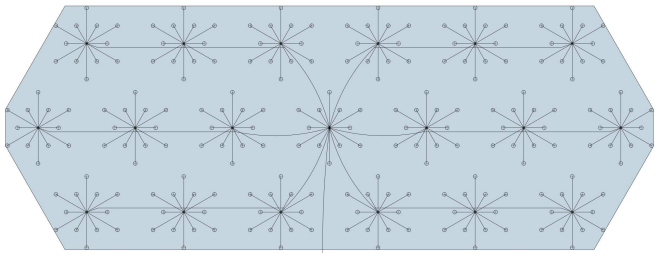

Fig. 3. Sample array layout.

V. MODEL

A. Assumptions and simplifications

The validation and simulation work is simplified to include only the floating cylindrical buoy hull, i.e., the submerged cylindrical PTO hull is excluded. This simplification is motivated by the complexity of simulating a two-bodied system with rope connection in CFD and the assumption of low influence of the PTO hull dynamics on the performance of the buoy.

B. Nonlinear Radiation-Diffraction Model

The open-source Boundary Element Method (BEM) solver NEMOH, [11], is used to generate the hydrodynamic coefficients for all the configurations and the nonlinear hydrodynamic model from the WEC-Sim [12] toolbox is used to perform the extensive number of simulations to optimize the system configuration.

C. CFD Model

The VOF-RANS model *interFoam* from the open-source finite volume framework OpenFOAM is used (OpenFOAM-v1912 as developed by ESI-OpenFOAM) [13]. OpenFOAM is based on 2nd-order cell-centred finite volumes on unstructured polyhedral cells. The hexahedral dominated meshes are created using the *snappyHexMesh* utility in OpenFOAM.

D. PTO Losses

The efficiency of all PTO components except the generators, are modelled as constants. Their values are obtained from suppliers and product datasheets. The ballscrew has 95% efficiency, pretension system – 99%, frequency converter – 98%. The generator losses are modelled with an efficiency map.

E. Viscous Drag

WEC-Sim accounts for the nonlinear Froude-Krylov (FK) and buoyancy force terms in the equations of motion. Nevertheless, there can still be significant mismatch between the model response and the real motion of the WEC. This mismatch arises mostly due to viscous drag losses from the large relative velocities, induced by energy-maximizing control strategies. In WEC-Sim viscous drag force is computed as proportional only to the velocity of the floater, i.e.,

$$\boldsymbol{F_v} = -\frac{1}{2}\rho \boldsymbol{C_d} \boldsymbol{A_d} |\boldsymbol{V}| \odot \boldsymbol{V} \tag{5}$$

where $\odot$ is the Hadamard (elementwise) product, $\boldsymbol{C_d} \in \mathfrak{R}^{3\times3}$ is a diagonal matrix with drag coefficient values in surge, heave, and pitch, $\boldsymbol{A_d} \in \mathfrak{R}^{3\times3}$ is a diagonal matrix with the respective characteristic areas and $\boldsymbol{V} \in \mathfrak{R}^{3\times1}$ is the respective buoy velocity vector. No modification is made to the original source code of WEC-Sim. Thus, the drag force formulation in WEC-Sim is used as it is.

The characteristic area is defined as the area of the orthographic projection of the object on a plane perpendicular to the direction of motion. In general, the characteristic area will change during motion of the device. However, in WEC-Sim the characteristic area is modelled as constant. The characteristic areas for all degrees of freedom are computed at the equilibrium position of the buoy using the definition found in OrcaFlex's documentation [14].

VI. Control

A. PRC

Due to its simplicity and numerical efficiency, the optimization study is performed with the polynomial reactive control strategy. PRC is a form of optimal reactive control, i.e. it controls the phase of the system in a similar way as the classical linear reactive control (LRC), but adds an extra degree of freedom to have better constraint handling. In this project a third-order polynomial is used for the reactive/spring term, and a first-order polynomial is used for the active/damping term. Moreover, the absolute PTO force is saturated at a certain maximum force, F_{max}. It can be mathematically expressed as

$$F_{pto} = \begin{cases} -F_{max}, & \boldsymbol{K^T\xi} \le -F_{max} \\ \boldsymbol{K^T\xi}, & |\boldsymbol{K^T\xi}| < F_{max} \\ F_{max}, & \boldsymbol{K^T\xi} \ge F_{max} \end{cases} \tag{6}$$

where $\boldsymbol{K} = \begin{bmatrix} K_{p_1} & K_{p_3} & K_{v_1} \end{bmatrix}^T$, $\boldsymbol{\xi} = [\xi \quad \xi^3 \quad \dot{\xi}]^T$ and ξ is the PTO displacement. Note that even orders of the polynomial are omitted due to the odd symmetry of the control force around the equilibrium.

The coefficients of the PRC during the validation and system optimization work are optimized for each sea state with the objective to maximize average export power by considering drivetrain efficiency and constraints. The constraints are included in the objective function by means of an exterior penalty function. The optimization of the control coefficients is done by the nonlinear gradient-based algorithm, *fmincon,* in MATLAB. The optimization algorithm for each sea state is initialized with the average of the optimal control coefficients of the neighbouring sea states to enable faster convergence of the optimization algorithm and to reduce the risk of the algorithm to end up at a local optimum.

B. Nonlinear MPC

In this work 1 DoF nonlinear model predictive control (MPC), as described in [5], is used with the optimal buoy configuration to estimate the potential performance improvement and LCoE reduction if a more advanced predictive control strategy is utilized. The objective function is nonlinear and is defined as a maximization of the output power by considering efficiency of the PTO. The internal model of the controller is linear. Moreover, perfect prediction of the liner FK force is assumed. Note that the simulated plant model is nonlinear, thus resulting in mismatch in dynamics and FK force between the plant and controller model. The MPC controller accounts for constraints of the system, such as PTO force and stroke, which are implemented as soft with the slack variable method. The prediction horizon of the controller is set to 5 s and the sampling period to 0.1 s. The nonlinear optimization problem is solved with the *fmincon* function with a sequential quadratic programming *(sqp)* algorithm.

VII. Results

A. Numerical Wave Tank Tests

1) Base Configuration

Two different identification experiments are performed with the base configuration: decay tests and regular wave tests with PTO force control activated.

I) Decay tests

Decay tests are performed in surge, heave and pitch, by displacing the buoy from its equilibrium position by 0.5 m, 0.5 m and 5°, respectively. Simulations are run for a duration of 10 s for heave and pitch, and for a duration of 50 s for surge. Symmetry of the hull and the domain is exploited to reduce the computational time. The convergence of the models is judged on the average oscillation period (T) and damping coefficient (γ) evaluated from the motion signals. Table VI shows the estimated periods and damping coefficients with the special discretization uncertainty for each DoF. It can be seen that the uncertainty with the densest mesh (M1) both in oscillation period and damping coefficient for all DoFs is below 5%. Thus, the simulations using the M1 mesh can be judged to be converged from a V&V perspective.

TABLE VI
ESTIMATED PERIODS AND DAMPING COEFFICIENTS IN SURGE (η_1), HEAVE (η_3) AND PITCH (η_5) AND ASSOCIATED SPATIAL DISCRETIZATION UNCERTAINTY FOR THE DECAY TESTS.

Grid	M4	M3	M2	M1
Number of cells	157872	307898	560198	3459304
T_{η_1} [s]	13.149	13.325	13.370	13.316
U_{η_1}	2.8 %	2.8 %	2.8 %	2.8 %
γ_{η_1} [-]	0.0123	0.0033	0.0030	0.0028
$U_{\gamma_{\eta_1}}$	3.6 %	2.4 %	1.7 %	0.7 %
T_{η_3} [s]	3.793	3.808	3.815	3.814
U_{η_3}	4.6 %	4.5 %	4.2 %	2.9 %
γ_{η_3} [-]	0.163	0.175	0.177	0.179
$U_{\gamma_{\eta_3}}$	6.2 %	4.1 %	2.9 %	1.2 %
T_{η_5} [s]	2.995	2.995	2.957	3.017
U_{η_5}	3.3 %	3.3 %	3.3 %	3.3 %
γ_{η_5} [-]	0.214	0.224	0.200	0.201
$U_{\gamma_{\eta_5}}$	7.1 %	6.5 %	6.1 %	4.9 %

II) Regular wave tests with control

The controlled 15m buoy is subjected to regular Stokes 5th order waves with a wave period of 10 s and a wave height of 4.5 m. Simulations are performed for a duration of 120 s with initial ramp-up time of 50 s. The buoy is controlled with PRC with coefficients optimally tuned for the particular regular wave. The uncertainty is estimated in terms of the normalized amplitude response in all DoFs. The results are presented in Table VII.

TABLE VII
ESTIMATED 1ST ORDER MOTION AMPLITUDES IN SURGE (η_1), HEAVE (η_3) AND PITCH (η_5) AND ASSOCIATED SPATIAL DISCRETIZATION UNCERTAINTY FOR THE CONTROLLED 15 M BUOY.

Grid	M4	M3	M2	M1
# cells	769312	978154	2294988	2965742
η_1 [m]	12.67	11.51	12.26	13.18
U_{η_1}	66.9 %	66.9 %	66.9 %	66.9 %
η_3 [m]	4.44	5.50	4.38	5.46
U_{η_3}	40.6 %	37.5 %	29.6 %	27.8 %
η_5 [o]	17.9	14.5	11.7	13.9
U_{η_5}	181.8 %	181.8 %	181.8 %	181.8 %

It is observed that the uncertainty for all DoFs is unacceptably large. This is a consequence of the presence of oscillatory convergence. This implies that denser meshes than the utilized ones are needed to have an acceptable spatial discretization uncertainty from the V&V perspective. Getting low numerical uncertainties for controlled WECs is difficult, see [15].

2) Optimal Configuration

CFD simulations are performed with the optimal buoy configuration subjected to regular Stokes 5th order waves with a wave period of 10 s and wave height of 4.5 m for a duration of 120 s with ramp-up time of 50 s. The buoy is controlled with PRC with coefficients optimally tuned for the particular regular wave. The uncertainty is estimated in terms of the normalized amplitude response in all DoFs and in the mean output power. The results are summarized in Table VIII. Again, it is observed that the uncertainty in motion amplitudes for all DoFs and in mean output power are unacceptably large due to oscillatory convergence. Even though the uncertainty in mean output power is unacceptable, we see that the difference in average output power between M2 and M1 is negligible. Therefore, the next densest meshes can safely be used in model calibration activities for the purpose of estimating average power and annual energy output.

TABLE VIII
ESTIMATED 1ST ORDER MOTION AMPLITUDES IN SURGE (η_1), HEAVE (η_3), PITCH (η_5) AND MEAN OUTPUT POWER ($\bar{P}$) AND ASSOCIATED SPATIAL DISCRETIZATION UNCERTAINTY FOR THE CONTROLLED 12 M BUOY.

Grid	M4	M3	M2	M1
# cells	756468	1014678	2893013	5295431
η_1 [m]	8.53	12.85	14.21	15.32
U_{η_1}	145.6 %	145.6 %	145.6 %	145.6 %
η_3 [m]	4.03	4.13	4.85	4.97
U_{η_3}	43.9 %	38.3 %	23.7 %	18.2 %
η_5 [°]	18.1	17.6	19.3	13.0
U_{η_5}	113.2 %	113.2 %	113.2 %	113.2 %
$\bar{P}$ [kW] [a]	588	683	694	698
$U_{\bar{P}}$	51.8 %	51.8 %	51.8 %	51.8 %

[a] Average using $t \in [60,\ 120]$ and estimated efficiency of 87.6%

B. Drag Calibration

Drag identification experiments are run in WEC-Sim to match the CFD simulations with the densest mesh.

1) Base Configuration

Drag calibration is initially performed on the base configuration using the motion responses from the performed CFD and WEC-Sim simulations. For the regular wave cases the initial 70 s in the responses is excluded when optimizing the drag coefficients, to avoid influence of the transient on the results. The optimally tuned drag coefficients for each experiment as well as the selected set of drag coefficients for the optimization study are shown in Table IX.

It is obvious that there is inconsistency in the drag coefficients obtained from different experiments. Despite these variations a single set of drag coefficients needs to be chosen. The recommendation for conservative choice

of drag coefficients in [16] is followed and the largest observed heave drag coefficient is chosen for the optimization study. Considering that larger drag coefficient in surge and pitch may cause suppression of parametric resonance [17], resulting in better overall performance, the surge and pitch drag coefficients are set to the mean value of all experiments.

TABLE IX
OPTIMALLY TUNED SET OF DRAG COEFFICIENTS FOR THE 15 M BUOY WITH DIFFERENT DRAG IDENTIFICATION EXPERIMENTS AND CHOSEN SET OF DRAG COEFFICIENT FOR THE OPTIMIZATION STUDY

	Surge	Heave	Pitch
Decay test	0.3560	1.2621	1.1665
Regular wave with control	1.3590	0 [a]	4.3146
Chosen for optimization study	0.8575	1.2621	2.7406

[a] The range of drag coefficients are constrained to positive values with motion objective function.

2) *Optimal Configuration*

The drag coefficients are recalibrated on the optimal configuration, initially with the motion objective function. Even though the recalibrated drag coefficients with the motion objective (Table XI) differed significantly from the utilized drag coefficients in the optimization study (Table IX), a good overall match between motion responses and average output power is observed. Nevertheless, for this regular wave scenario the average power in WEC-Sim is found to be approximately 11% lower than the one from the CFD model, see Table X. This implies that the drag coefficients optimized to minimize the least square error

TABLE X
COMPARISON OF THE AVERAGE OUTPUT POWER OBTAINED WITH WEC-SIM AND CFD MODELS

	C_d, base config.	C_d, motion obj.	CFD
Avg power, [kW]	652.2	656.9	694.0

between the motion responses, does not guarantee minimum error in the average output power between the WEC-Sim and CFD models. To guarantee minimum error between the average output powers in WEC-Sim and in CFD, the drag coefficients are instead calibrated with the power objective function. Since the influence of the pitch drag coefficient on the mean output power is low, the optimization algorithm fails at choosing a reasonable pitch drag value. Therefore, the pitch drag value is fixed to the one obtained with the motion objective function.

The obtained set of drag coefficients with the power objective is shown in Table XI, along with the one obtained with the motion objective. Once again significant difference between the drag coefficients is present. Note that the heave drag coefficient is negative, which is not technically incorrect since the drag coefficients are descriptors of all the unmodelled dynamics, irrespective of their source and nature, rather than coefficients in the physical sense of drag. This objective function gives 0% error between the mean output powers with WEC-Sim and CFD, but larger weighted average error between the motion responses. Nevertheless, no significant visual difference is observed between the motion responses obtained with these sets of drag-coefficients.

TABLE XI
OPTIMALLY TUNED DRAG COEFFICIENTS FOR THE 12 M HULL WITH THE MOTION AND POWER OBJECTIVE FUNCTIONS

	Surge	Heave	Pitch
Motion objective	3.472	0.632	1.437
Power objective	2.129	-0.711	1.437

C. *Optimization Study*

The optimization is performed in two stages. The design wave resource is chosen to be the Belmullet site.

1) *First Stage*

At the first stage the score, defined as weighted average power per total CoGs, is computed for each configuration, see Table XII, with the parameters defined in Table XIII. The maximum tether force is equal to the force required to fully submerge the buoy. The 12 m hull is the configuration with the highest score, followed by the 15 m hull.

Note that the optimal configuration might differ depending on the sea site. However, the optimal configurations found in the Belmullet site produced nearly the same score as the optimal configuration found for other sites. Thus, the optimal configuration is found to be less sensitive to the wave resource.

2) *Second Stage*

TABLE XII
WEIGHTED AVERAGE POWER PER COGS [KW/M€]

		V [m3]	300		350			400						450						500						550						600			650			700			750	
		m [ton]	25	50	25	50	100	25	50	75	100	125	150	25	50	75	100	125	150	50	75	100	125	150	50	100	125	150	50	100	150	50	100	150	50	100	150	100	150
D [m]	F [MN]	s [m] / T [MN]	2.8	2.5	3.3	3	2.5	3.8	3.5	3.3	3	2.8	2.5	4.3	4	3.8	3.5	3.3	3	4.5	4.3	4	3.8	3.5	5	4.5	4.3	4	5.5	5	4.5	6	5.5	5	6.5	6	5.5	6.5	6
9	1	5	177	175	170	170		158	162					152	152																											
9	1	6	178		171				165																																	
9	1	7			167				169																																	
9	1.5	5												134	133		128			128		123			123	115																
9	1.5	6												138	138																											
9	1.5	7												139	139																											
12	1	5		184		191	186		184	192	193	191	179		176	180	188	192	188		173	178	184	181			176	172														
12	1	6							179								185																									
12	1	7							173								178																									
12	1.5	5													180										171	175		168	165			158	161	160								
12	1.5	6													177										165																	
12	1.5	7													169										157																	
12	2	5																		159					160	155			155	154		149	150			143						
12	2	6																											149				144									
12	2	7																											141				135									
15	1.5	4																								181								180								
15	1.5	5													166		165		126						160	177		176					166	171								
15	1.5	6																								168								163								
15	2	5																							158	162			155	164	157	150	161	160	145	157	156	167	152
15	2	6																												154			151				146		142

At the second stage of the optimization, the configurations with the highest score for each buoy width are benchmarked in terms of LCoE. For this purpose, annual simulations are run with each configuration to calculate annual energy yield. The power output is saturated at the device rating, which is selected based on the average power in the design sea state Hs = 4.75 m, Te = 9.5 s. The device rating also gives the number of units per 100 MW installed capacity for each configuration, which is used to design the array configuration. The results for the three configurations in the Belmullet site are summarized in Table XIII. The optimal configuration is found to be the 12 m hull, as predicted by the scoring method at the first stage of the optimization. However, at this stage the runner up is the 9 m hull. This is due the scale effects predicted by the learning curve methodology, which favours smaller size devices. The scale effects are however still not considered by the CoGs scaling methodology, which indicate that the 15-meter hull configuration would show the best economy in the longer run when the volume effects reduce.

TABLE XIII
BENCHMARK OF THE THREE CONFIGURATIONS RATED AT SEA STATE HS=4.75M, TE=9.5S IN BELMULLET

	Configurations			
Device specification	**9 m**	**12 m**	**15 m**	
Device rating	298	333	397	kW
Buoy diameter [D]	9	12	15	M
Buoy volume [V]	300	400	550	m3
Buoy mass [m]	25	100	100	ton
PTO active control force	1	1	1.5	MN
Total tether force [T]	2.75	3	4.5	MN
PTO stroke length [S]	6	5	5	m
Array specification				
Nr WEC´s	336	300	252	units
Capacity factor	50%	52%	54%	
Annual energy per WEC	1 307	1 531	1 880	MWh
Parameters				
CAPEX	0.8	0.88	1.28	m€
OPEX	0.064	0.07	0.102	m€/y
Lifetime	20	20	20	y
Discount rate	10%	10%	10%	
LCoE	**121.1**	**113.4**	**134.3**	€/MWh

3) *Optimal Configuration*

Annual simulations are run with the optimal 12 m hull, with the drag coefficients recalibrated with the motion and power objective functions. Fig. 4 shows a comparison of the annual energy and LCoE with both objective functions. Power objective function produces 3-8% more annual energy and lower LCoE compared to the motion objective, for the same device rating. Note that these LCoE values differ from the values in Table XIII, due to the recalibrated drag coefficients.

The 1 DoF MPC cannot be used together with the nonlinear 3 DoF model due to the great mismatch between controller and plant model dynamics, which resulted in poor performance. Moreover, implementing a 3 DoF MPC is outside the scope of the project. To estimate the potential LCoE numbers with a 3 DoF MPC, annual simulations with both PRC and 1 DoF MPC are run with a nonlinear heave model of the system. The ratio between annual energy yield with 1 DoF MPC and PRC is applied to the results from the nonlinear 3 DoF PRC model to estimate the power matrix with 3 DoF MPC. MPC is found to increase the annual output with 17-34%

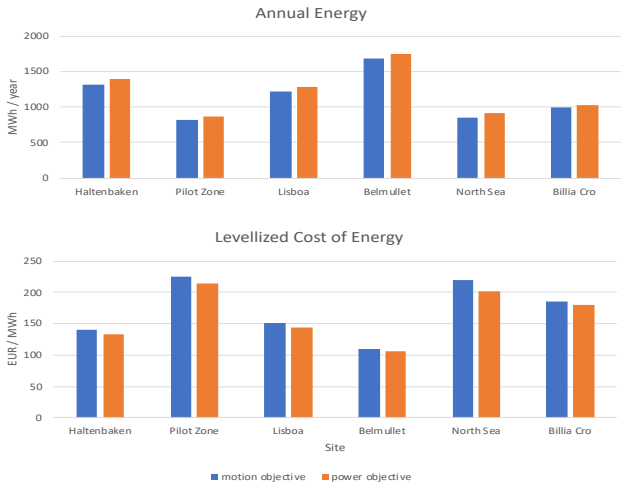

Fig. 4. Annual energy and LCoE comparison with 12 m between the set of drag coefficients, tuned using motion and power objective.

depending on the site. It is worth mentioning that MPC is also much more effective in reducing violations of the constraints of the system. However, it requires 4-5 second accurate wave prediction. The annual energy and LCoE numbers for all sites are shown in Fig. 5 (with drag coefficients tuned with the power objective).

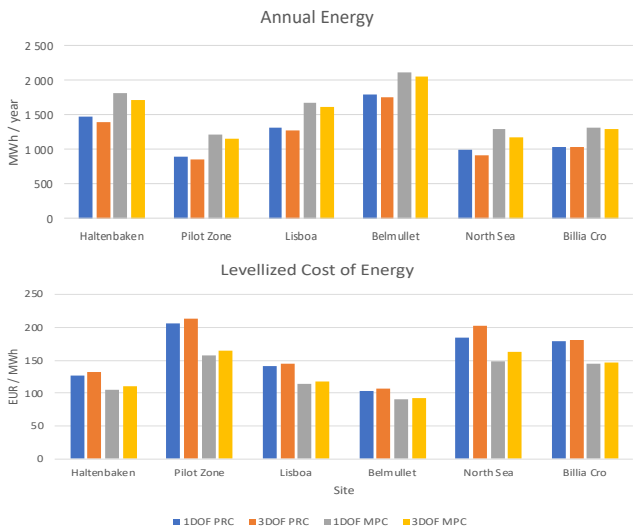

Fig. 5. Annual energy and LCoE comparison between the different wave resources.

VIII. DISCUSSION AND CONCLUSION

An optimization method has been developed and shown to be effective in identifying the configuration of OHT's wave energy converter InfintiyWEC with the lowest LCoE. The method is based on scaling costs on a component level, using scale factors applied on the change of the functional parameters they are affected by. It enables setting scale factors for a component that accounts for, for instance, the level of machining relative

to the use of material. This highlights the inaccuracy of using metrics like CAPEX/ton, since for instance reducing weight of a component does not automatically result in lower CAPEX. Scaling costs based on a defined cost base line and the change in geometry and load on each component in the system is a more accurate approach to long-term cost development.

Key findings from the optimization study are that configurations using lower PTO force give higher score and that the optimal volume of the buoy hull must be well balanced in relation to the control force in the PTO. It is also noted that the optimal configuration does not have the lightest possible mass of the buoy, it is instead 100 ton, indicating that low-cost concrete material can be a suitable option for the hull instead of light-weight materials. The result of the study is an LCoE between 106 – 225 EUR/MWh with the nonpredictive control strategy (PRC) and 93 – 162 EUR/MWh with the predictive control strategy (MPC), for the n:th unit at 100 MW installed capacity.

The validation of the simulation model with numerical tank testing is not as straightforward as anticipated. The CFD simulations in a regular wave scenario with the control force active is not converged in a V&V sense. This implies that significantly larger mesh density is needed to achieve acceptable spatial discretization. Nevertheless, convergence of the average output power with the 12 m buoy is observed already with the next densest mesh.

It is observed that the values of the drag coefficients differ significantly between the evaluated cases. This is not surprising, since the drag coefficients in fact are descriptors of all the unmodelled effects and large variations will occur when the flow conditions are significantly changed. This implies that the drag coefficients need to be tuned for different flow conditions / sea states or the WEC-Sim model needs to be improved to better capture the unmodelled dynamics.

The calibration of the optimal WEC configuration is done using both a motion and a power objective. It is observed that the set of drag coefficients obtained with the motion objective function underestimates the performance of the WEC by 11% in the regular wave the drag coefficients are tuned in. This resulted in 3-8% difference in the annual energy yield and thus LCoE.

Despite the encountered challenges with model validation using numerical tank testing, the method is found to be very useful. The validation can be done in a controlled, repeatable environment at full scale, thus scale effects and all uncertainties in wave tank testing are avoided. All parameters can easily be investigated in a cost effective and time efficient way unlike physical testing. Physical tank testing may still be required but can now be performed for the purpose of validating an optimized system, rather than for the purpose of providing parameters for the optimization itself.

REFERENCES

[1] A. Babarit, J. Hals, M. J. Muliawan, A. Kurniawan, T. Moan, and J. Krokstad, "Numerical benchmarking study of a selection of wave energy converters", *Renew. Energy*, vol. 41, pp. 44–63, 2012. DOI: 10.1016/j.renene.2011.10.002, [Online].

[2] N.Y. Sergiienko, A. Rafiee, B.S. Cazzolato, B. Ding, M. Arjomandi, "Feasibility study of the three-tether axisymmetric wave energy converter", *Ocean Engineering*, vol. 150, pp. 221-233, 2018. DOI: 10.1016/j.oceaneng.2017.12.055, [Online].

[3] A. De Andres, J. Maillet, J. H. Todalshaug, P. Möller, D. Bould, and H. Jeffrey, "Techno-Economic Related Metrics for a Wave Energy Converters Feasibility Assessment", *Sustainability*, vol. 8, pp. 1109, 2016. DOI: 10.3390/su8111109, [Online].

[4] S. Lundberg, "Performance comparison of wind park configurations", Phd thesis, Department of Electric Power Engineering, Chalmers University of Technology, Chalmers University of Technology, 2003, [Online].

[5] A. Rashid, M. Sidenmark, "Numerical Benchmarking of selected Efficiency-Aware Reactive Control Strategies on the InfinityWEC Wave Energy Converter", in *13th European Wave and Tidal Energy Conference (EWTEC)*, 1-6 September 2019, Naples, Italy, [Online].

[6] OES-IEA, "An International Evaluation and Guidance Framework for Ocean Energy Technology", 2021, [Online]

[7] OES-IEA, "International Levelised Cost of Energy for Ocean Energy Technologies", 2015, [Online]

[8] J. Todalshaug, G. Ásgeirsson, E. Hjálmarsson, J. Maillet, Jéromine, P. Möller, P. Pires, M. Guerinel, Matthieu, M. Lopes, (2016). "Tank testing of an inherently phase-controlled Wave Energy Converter", *International Journal of Marine Energy*, 15. 10.1016/j.ijome.2016.04.007, [Online]

[9] C. Windt, N. Faedo, D. García-Violini, Y. Peña-Sanchez Y, J. Davidson, F. Ferri, JV. Ringwood, "Validation of a CFD-Based Numerical Wave Tank Model of the 1/20th Scale Wavestar Wave Energy Converter". *Fluids*. 2020; 5(3):112. https://doi.org/10.3390/fluids5030112, [Online]

[10] L. Eca and M. Hoekstra, "A procedure for the estimation of the numerical uncertainty of CFD calculations based on grid refinement studies", *Journal of Computational Physics*, vol. 262, pp. 104 – 130, 2014. DOI: 10.1016/j.jcp.2014.01.006, [Online]

[11] A. Babarit, G. Delhommeau, "Theoretical and numerical aspects of the open-source BEM solver NEMOH", *Proceedings of the 11th European Wave and Tidal Energy Conference (EWTEC)*, 6–11 September 2015, Nantes, France, [Online]

[12] Y. Yu, M. Lawson, K. Ruehl, "Development and demonstration of the WEC-Sim wave energy converter simulation tool", *Proceedings of the 2nd marine energy technology symposium*, 15–17 April 2014, Seattle, WA.

[13] OpenFOAM. http://www.openfoam.com, 2019, [Online]

[14] Orcina Ltd. Orcaflex online documentation (version 11.0d). [Online]

[15] W. Wang, M. Wu, J. Palm, C. Eskilsson. "Estimation of numerical uncertainty in CFD simulations of a passively controlled wave energy converter", *Proc. Inst. Mech. Eng., Part M: Journal of Engineering for the Maritime Environment*, 2018, Vol. 232(1): 71-84.

[16] G. Giuseppe, J. Ringwood, "Consistency of Viscous Drag Identification Tests for Wave Energy Applications", in *12th European Wave and Tidal Energy Conference (EWTEC)*, 27th Aug-1 Sept 2017, Cork, Ireland, [Online].

[17] G. Giorgi, R. Gomes, G. Bracco, G. Mattiazzo, "Numerical investigation of parametric resonance due to hydrodynamic coupling in a realistic wave energy converter", *Nonlinear Dynamics*, 2020, 101. 10.1007/s11071-020-05739-8.